

Strong adhesion of water to CeO₂(111)

S Gritschneider¹, Y Iwasawa² and M Reichling¹

¹ Fachbereich Physik, Universität Osnabrück, Barbarastraße 7, 49076 Osnabrück, Germany

² Department of Chemistry, University of Tokyo, Hongo, Bunkyo-ku, Tokyo 113-0033, Japan

E-mail: reichling@uos.de

Received 27 October 2006, in final form 4 December 2006

Published 21 December 2006

Online at stacks.iop.org/Nano/18/044025

Abstract

The adsorption of water molecules on a stoichiometric CeO₂(111) surface at room temperature is studied with dynamic scanning force microscopy. Atomic resolution imaging reveals spontaneous adsorption as well as deposition of molecules by the tip of the force microscope. Water molecules localize exclusively on one type of site that is associated with the cerium ion sub-lattice and stick to the surface with an estimated surface diffusion barrier of 1 eV. Occasionally adsorbates are moved laterally across the cerium sub-lattice by the action of the scanning tip.

(Some figures in this article are in colour only in the electronic version)

 This article features online multimedia enhancements

Water adsorption is one of the most fundamental processes in surface physics and has been extensively studied since the respective analytical methods have been available [1–3]. The details of the adsorption mechanism and the wetting behaviour are determined by a complex interplay between several factors such as adsorption energy, surface geometry, kinetic barriers, and subtleties of the investigated surface [1]. A crucial question in this context is whether the adsorption is associative (molecular) or dissociative, but there is no simple way to determine this *a priori* based on simple model considerations. For the well studied class of metallic surfaces, it has been established that there are two groups of metals, one featuring molecular and the other one dissociative adsorption of water, however, there is still a controversial discussion about some cases of conflicting experimental findings (see [2] for an overview). Clean and stoichiometric surfaces of bulk oxides have been investigated in much less detail, mainly due to experimental peculiarities. Most available evidence is based on spatially averaging spectroscopic methods or theoretical simulation [4, 5] as only since recently, atomic structures on insulating oxides can directly be revealed by dynamic force microscopy [6].

Here, we investigate the adsorption of water molecules at the stoichiometric (111) surface of ceria (CeO₂, cerium dioxide), a material used in various industrial applications because of its remarkable catalytic properties that are mostly based on the facile oxidation and reduction of surface and bulk cations and the related high oxygen storage capacity [7]. Water

adsorption to this surface has been studied with photoelectron spectroscopy and thermal desorption spectroscopy predicting molecular adsorption [4] and yielding a desorption temperature of 320 K for 0.05 ML coverage with a shift towards 200 K for 1 ML coverage (the adsorption energy at 1 ML is higher than 0.51 eV).

In our studies, we apply dynamic scanning force microscopy (SFM) operated in the non-contact mode (nc-AFM) at room temperature in ultra-high vacuum (UHV). This technique readily allows high quality atomic scale imaging of CeO₂(111) as well as adsorbates on this surface [8]. In a series of consecutively recorded images of the same surface area that were performed during different exposures of the surface to water, we observe individual adsorption events and find that water adsorption is strongly enhanced under the influence of the scanning tip. We demonstrate that water adsorption occurs exclusively at one well defined surface site that we associate with the cerium ion sub-lattice and roughly estimate a barrier of 0.98 eV for diffusion across this sub-lattice.

Experiments are performed with the same equipment, sample preparation and scanning techniques used in our previous study of the ceria surface [8]. Cantilevers have a resonance frequency of 60–70 kHz and are excited to oscillation at a constant amplitude of 35 nm. To obtain atomically resolved images, the surface is scanned in the constant height mode with a scanning speed of 3 lines s⁻¹, while variations in the detuning of the cantilever oscillation are recorded as a measure of the tip–sample interaction. A stronger

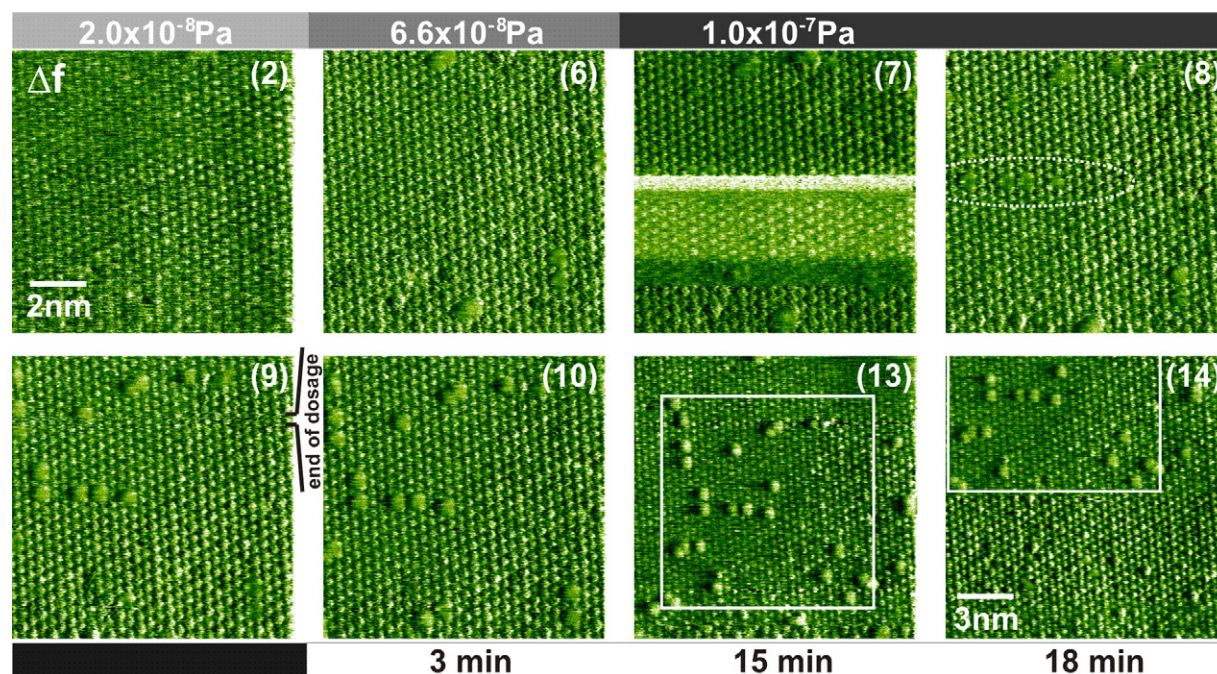


Figure 1. Series 1 representing atomically resolved images of a stoichiometric $\text{CeO}_2(111)$ surface during water exposure. The series comprises sixteen consecutively recorded frames, of which eight are shown in the figure. For each frame the water partial pressure is given in the grey shaded bar above or below the frame. The frame number is given as a number in brackets. The clean surface is preserved at low exposure rates and first molecules adsorb at the time recording frame (6) corresponding to a dosage of 0.3 L. Tip instabilities during recording frame (7) result in the deposition of four water adsorbates marked in the following frame by an ellipse. The molecules adsorb at threefold hollow sites resulting in their characteristic triangular appearance. By increasing the scan range in frame (13) and shifting the field of view in frame (14), it becomes obvious that adsorption is strongly enhanced by the presence of the scanning tip.

attractive interaction between the tip and the surface results in a higher negative detuning that is represented as a brighter contrast in the SFM images shown here. The atomic contrast pattern resulting from a perfect surface consists of hexagonally arranged circular features that can be assigned to the surface terminating oxygen ions [9]. By preparation under very clean conditions (partial pressures of residual gas components such as CO or H_2O are below 1×10^{-9} Pa), we succeed in preparing surfaces that are free of defects in the scanned area in the beginning of each experimental series. Ultra-clean Milli-Q water, further purified by several freeze–pump–thaw cycles, is introduced into the UHV chamber via a high-precision leak valve during scanning. The operation of the valve may result in a slight disturbance of the measurement that can be identified in images (see e.g. ‘end of dosage’ in figure 1). The residual gas composition and gas dosage is monitored with a quadrupole mass analyser. We use Nanosensors cantilevers (PPP-QFMR), which were annealed at 120°C prior to experiments. After such treatment, the silicon tip can be expected to be covered by the original native oxide layer, which itself is most probably partially hydroxylated [10]. The three series of measurements shown here are representative of a larger number of similar experiments where exactly the same phenomena have been observed.

In a first series of 16 consecutively recorded frames, we start with an initially clean surface area of $10 \times 10 \text{ nm}^2$ and increase the water partial pressure from the residual gas level of 5×10^{-10} to 1×10^{-7} Pa in three steps exposing the surface to a total dosage of 0.8 L (Langmuir). Water dosage

is stopped after 30 min while we continue scanning. Eight representative frames from this series representing several stages of water adsorption are compiled in figure 1, where the frame numbers are given in the upper right corner of the respective frame. Exposure to the initial water partial pressure of 5×10^{-8} Pa converts into a dosage of 0.03 L/frame. No adsorption is observed during recording of the first four frames; as a representative result we show frame (2) exhibiting a completely clean and stoichiometric surface. In this and similar frames recorded during water exposure, we find, however, slight instability in imaging and irregularity in contrast formation that we attribute to a disturbance from water molecules interacting with the scanning tip. Starting with frame (4), we increase the water pressure to 6.6×10^{-8} Pa resulting in a dosage rate of 0.1 L/frame. When recording frame (6), the water exposure amounts to 0.3 L and we observe the formation of a few protrusions appearing on the regular atomic grid. We associate these protrusions with water molecules and justify this below after discussing all available experimental evidence. Before recording frame (7), we increase the water pressure to 1×10^{-7} Pa resulting in a dosage rate of 0.15 L/frame. Apparently, the higher water pressure causes severe tip instability in the lower half of frame (7), culminating in a region where atomic contrast is completely lost for about 30 scan lines. Afterwards, atomic contrast is re-gained, without a significant difference in imaging quality compared to the contrast at the beginning of the frame. This type of severe instability is a characteristic feature of water exposure occurring when the water pressure

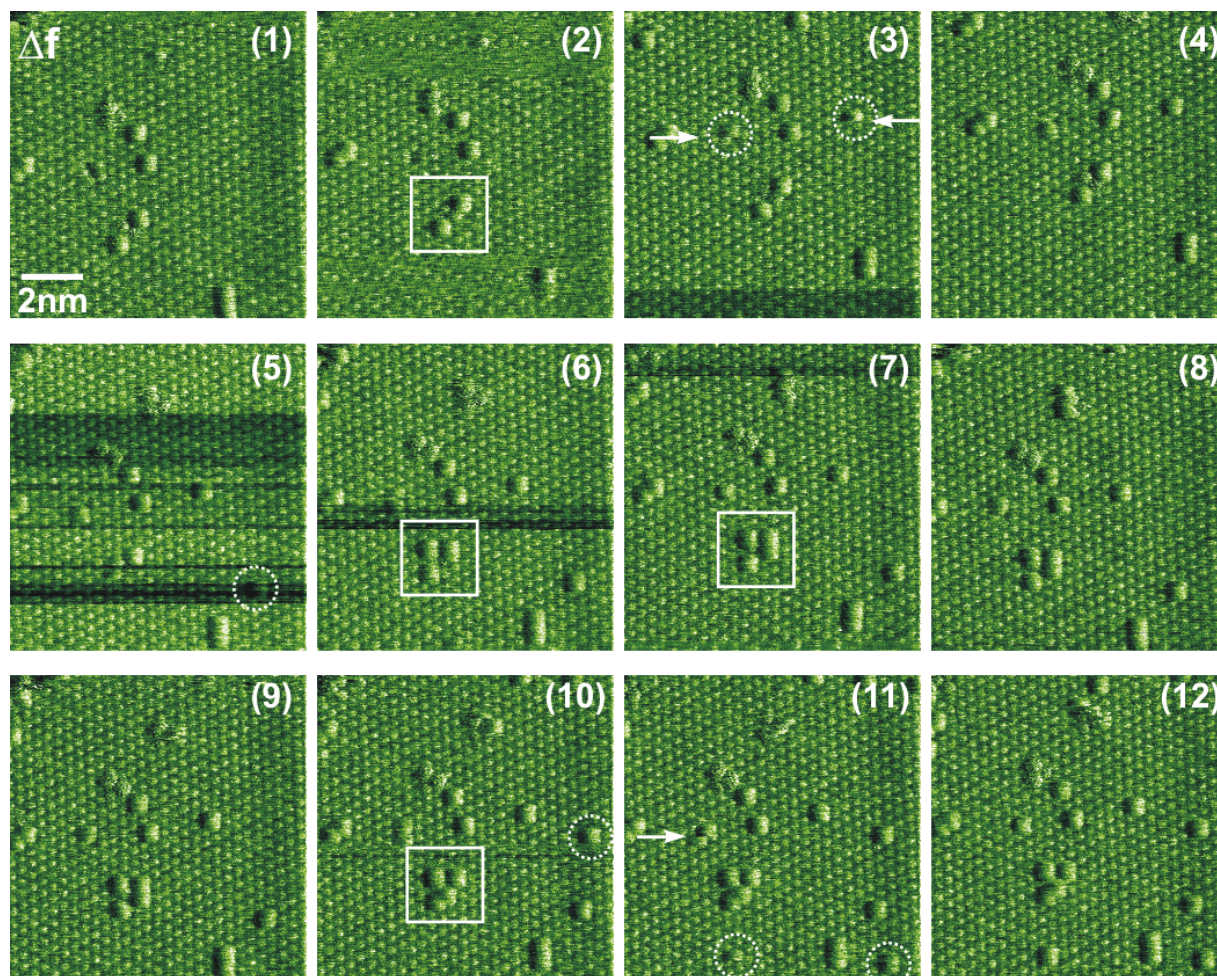


Figure 2. Series 2 with 12 consecutively recorded images of a surface which from the beginning is already covered by water adsorbates due to 6 h of exposure at a water partial pressure of 1×10^{-8} Pa that is preserved throughout the entire measurement. Dotted circles point to newly adsorbed molecules. Events of strong interaction between tip and adsorbates resulting in adsorption or movement of molecules are marked by arrows in frames (3) and (11), respectively. The group marked by the square in several frames shows increased adsorption and diffusion activity and the last configuration as in frame (10) is depicted in more detail in figure 3.

exceeds a critical level of about 1×10^{-7} Pa and is not observed when dosing the surface with other gases such as O_2 or CO at even higher pressure levels of up to 5×10^{-6} Pa. This points to the strong interaction of water with both, the ceria surface and the scanning tip. In fact, such interactions result in the tip-induced deposition of molecules as apparent in the area marked by the ellipse in frame (8). The configuration of four water molecules deposited exactly in the region of severe instability of frame (7) appears with low contrast and as partially transparent features in frame (8), probably due to a slight variation in tip–surface distance, but they can clearly be observed as strong contrast features in a stable configuration in all following frames. In frames (8) and (9), we also observe molecules appearing without any noticeable influence on the scan process and attribute them to spontaneous adsorption events. After stopping gas exposure, we continue imaging for 12 min, enlarge the scanning area to 15×15 nm² starting from frame (13) and shift the field of view downwards before recording frame (14). In the last six frames of the series, we observe a few further adsorption events appearing at a low rate corresponding to the strongly reduced water partial

pressure. The most striking observation best seen in frame (14) is, however, that the density of molecules adsorbed within the square of the previously scanned area is much larger than the density of molecules adsorbed in the outer region. The somewhat uneven, but nonrecurring, contrast in the lower half of the frame should not be confused with defects, but is again a result of an instability in the measurement probably due to residual water molecules attached to the tip. From an analysis of the density of defects in scanned and unperturbed areas, we draw the conclusion that the average adsorption rate of about 15×10^{-3} s⁻¹ during scanning is six times higher than the rate on the unperturbed surface. Obviously, adsorption is strongly promoted by the presence of the scanning tip acting as a reactive centre for water chemisorption [2, 10] and transferring water molecules onto the surface. Scanning experiments performed during exposure to water partial pressures above 1×10^{-7} Pa turned out to be a very risky manoeuvre, repeatedly resulting in severe scanning instability, a complete loss of atomic contrast or even a tip crash.

In a second series of 12 consecutively recorded frames, shown in figure 2, we investigate the evolution of water

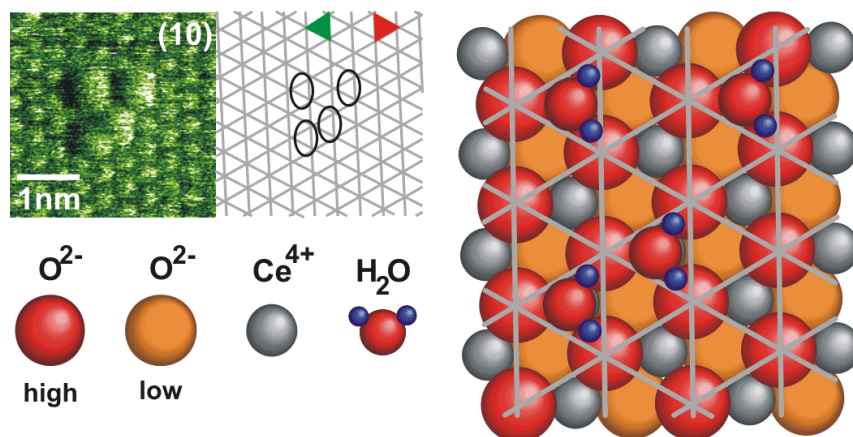


Figure 3. Detailed view of a group of adsorbates from series 2. Next to the original image, a hexagonal (1×1) mesh defines the oxygen sub-lattice with its crossing points. The group consists of four water molecules and the surface scheme at the right illustrates the position of the defects with respect to the subjacent lattice as observed in frame 10. Note that water molecules exclusively adsorb on one kind of lattice site, a three fold hollow position, connecting three top layer oxygen ions to protruding triangles pointing to the left-hand side. These lattice sites are associated with the cationic sub-lattice marked with the green triangle. The red triangle marks the lower anion sub-lattice, with sites never occupied by water adsorbates.

adsorbates on the surface exposed to a constant water partial pressure of 1×10^{-8} Pa before and during imaging. The series was started six hours after sample preparation resulting in an initial water exposure of 1.5 L. Already in the first frame we detect a significant number of adsorbates yielding evidence that water molecules also adsorb if the tip is not present. The defect density present in the first frame due to the initial dosage accounts to 1.4% of a monolayer, corresponding to an adsorption rate of $3.7 \times 10^{-4} \text{ s}^{-1}$. During the 60 min of acquisition time of the complete series, the defect density reaches 3% of a monolayer, i.e. twice the initial value. This corresponds to an increase of the adsorption rate by a factor of 7 to $2.5 \times 10^{-3} \text{ s}^{-1}$. This value is well in line with the rate determined for series 1 when considering the different water exposure. Adsorption events are marked by dotted circles in figure 2. As observed in frame (3), only the upper half of the two new adsorbates are visible indicating that the molecules adsorb while the tip is sampling along the scan lines marked by arrows. In the range of coverages observed here, most of the water is randomly spread across the surface, while some of the molecules form dimers or small groups. The most prominent group, highlighted by the square frames, initially consists of two molecules. During the experiment, two more molecules attach and finally one of the molecules changes its position. For a more detailed analysis of adsorption sites, the last configuration of this group, as apparent in frame (10), is magnified in figure 3. The adsorbates are schematically depicted in a sketch placed next to the original image that includes a (1×1)-mesh with crossing points indicating the position of oxygen ions of the surface terminating layer. Analysing many images similar to the one discussed here, we find that the apparent shape of water may vary from triangular to circular or an elongated feature, however, all adsorbates are exclusively centred at hollow positions marked by the green triangle. Principally, the centre point of these hollow positions could either be the lattice site of a cerium ion or the one of a lower oxygen ion of the terminating O–Ce–O triple layer. However, by imaging the surface at very close tip-sample

distances, a honeycomb-like contrast pattern is obtained that allows unambiguous determination of the position of cerium sites [11]. Imaging a water contaminated area in this mode shows that water molecules adsorb exclusively at cerium sites, and this is also plausible because water as a polar molecule can be expected to bind with its partially negative oxygen to positive cerium sites. According to this consideration, adsorbates are schematically depicted in the sketch shown in figure 3, where we also suggest a certain orientation for the water molecules. In that way, water molecules act as markers of the cationic sub-lattice and water adsorption allows an indirect but reliable determination of the sub-lattices in the surface. While the main binding interaction will occur between the surface cation and the water oxygen, there might be additional binding to the adjacent surface oxygen via hydrogen bridges as the $\text{O}_{\text{H}_2\text{O}}\text{--O}_{\text{surf}}$ distance is comparable to that of hexagonal ice [4]. The absence of any lateral order indicates that there is no significant hydrogen bonding between the water molecules, and that the adsorption process is dominated by the strong interaction of water with the substrate.

The adsorption/desorption energy is not directly accessible in the present experiments, but we can roughly determine a diffusion barrier from the diffusion events observed in series 2. Similar to adsorption, diffusion is also sometimes tip induced, resulting in the characteristic appearance of halved adsorbates, as observed for the marked (see arrow) defect in frame (11) of figure 2. However, most of the diffusion events such as the one in the last step described for the square framed group in figure 2 do not show any sign of being induced by the tip. More events can be identified in the movie composed from the complete series that is provided as supporting online material (available at stacks.iop.org/Nano/18/044025). The rate equation $\nu_d = \nu_0 \cdot e^{-\Delta E_d/k_B T}$ allows determination of the diffusion barrier ΔE_d from the observed diffusion frequency ν_d and a given attempt frequency ν_0 . The diffusion frequency for a single molecule is calculated as $\nu_d = \frac{n_d}{a \times \Delta t} = \frac{5}{15 \times 3600 \text{ s}} = 9.2 \times 10^{-5} \text{ s}^{-1}$, with n_d being the number of observed diffusion events and a being the average number of adsorbates at the

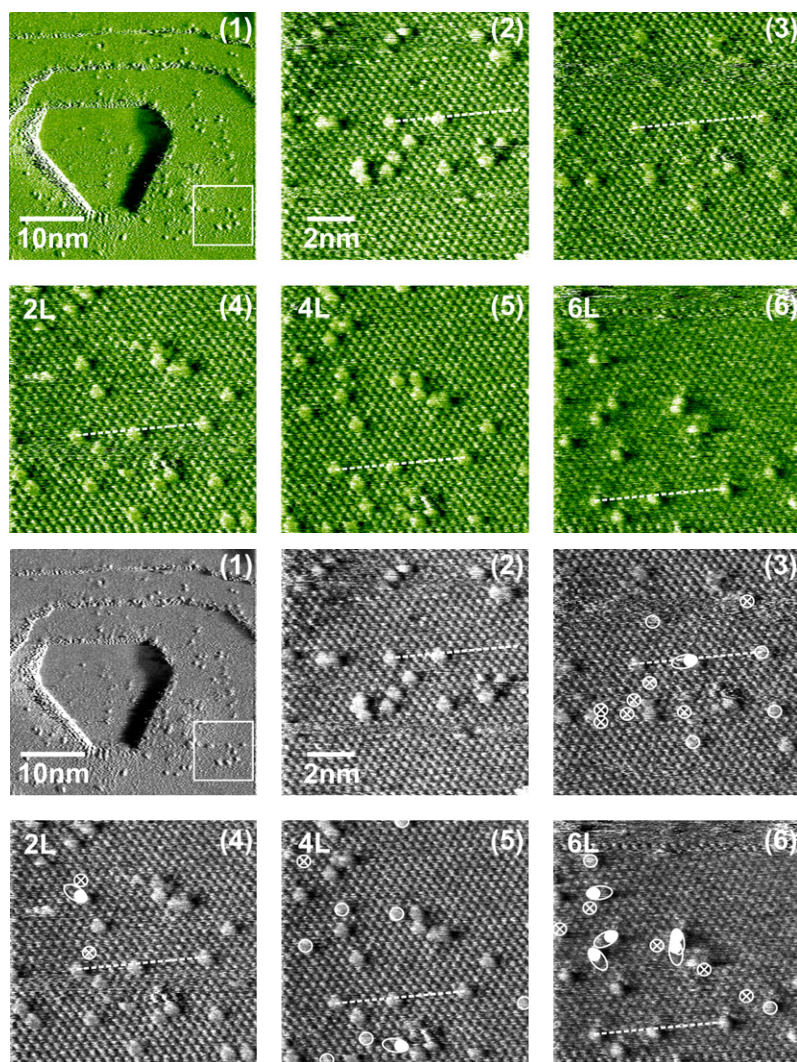


Figure 4. Series 3 demonstrating adsorption, desorption and tip-induced diffusion of water molecules. The surface is exposed to a small amount of water (0.1 L) and a large amount of molecular oxygen (6 L). All observed reactions or adsorption events involve water molecules and none could be related to oxygen. For clarity, we marked each event in the black-and-white reproduction of the original measurement. Additional water molecules are indicated by open circles, disappearing molecules are marked by crossed circles and diffusing molecules by ellipses. In frames (3) and (6) tip instabilities have detrimental effect on the contrast quality, and also seem to induce water diffusion or disappearance.

surface during the duration Δt of the experiment, one hour in this case. Assuming the phonon frequency of water of 10^{13} Hz as a plausible attempt frequency [12], we calculate a diffusion barrier of 0.98 eV. By definition, the actual adsorption energy is equal or larger than the diffusion energy determined here, which is already significantly higher than typical adsorption energies reported in the literature [1, 4]. As it cannot be excluded that some of the diffusion events are tip induced, the actual diffusion barrier might even be higher, and the value of 0.98 eV should, therefore, be understood as a lower limit, revealing that water adsorption to the stoichiometric $\text{CeO}_2(111)$ surface is remarkably strong.

In figure 4, we show a third series of measurements performed to demonstrate dynamic effects during combined water and oxygen dosage. Frame (1) is a survey image demonstrating the density and distribution of adsorbates at step edges and on terraces, while frames (2) to (6) are a series of images consecutively taken at a selected area of frame (1).

The water partial pressure was 1.5×10^{-8} Pa during the entire series, resulting in a final dose of 0.1 L water at the end of the series. To study possible effects of oxygen on the defective surface, we additionally dosed the surface during frame (4) to (6) with molecular oxygen at a pressure of 1×10^{-6} Pa, resulting in a final dose of 6 L oxygen at the end of the series. However, in this, like in most other measurements involving the dosage of molecular oxygen, we could not find any effect that could be ascribed to oxygen exposure. Therefore, all results reported here are solely due the much smaller exposure of the surface to water. Frame (1) demonstrates that water molecules are adsorbed randomly on flat terraces, where they appear as single species or in small clusters. Water adsorption is also found at step edges, where molecules mostly adsorb at the upper terrace. This indicates that step edges provide adsorption sites, however, due to the small mobility of water on the surface, step edges are not strongly decorated with water molecules.

Frames (2) to (6) represent the same repetitively scanned surface area where the apparent shift of structures is a result of thermal drift that is unavoidable for room temperature measurements. As a guide to the eye, we have marked a group of three water molecules drifting downwards. In these frames, we observe the adsorption, desorption and re-arrangement of water molecules. For clarity, we marked each event in the black-and-white reproduction of the images in the lower part of figure 4. Adsorption of water molecules is marked by small open circles, disappearing water molecules are marked by crossed circles and a re-arrangement of water molecules is marked by ellipses and filled circles. As the main observation, we note that water molecules appear at random positions on the scanned surface area, indicating spontaneous adsorption, and only in frames (3) and (6) an increased number of molecules disappears or is shifted. We also note for these frames, especially for frame (6), that tip instabilities discernible by horizontal stripes have a detrimental influence on the quality of the atomic contrast. Most probably this is a consequence of an atomic re-arrangement of the tip terminating cluster, which in turn could be responsible for increased interaction between the tip and adsorbed molecules, resulting in their displacement.

Principally, the species we observe upon water dosage could be molecular water as well as a hydroxyl group adsorbed onto the surface, as both species are expected to coordinate to cation sites. However, water dissociation would result in the formation of a negatively charged hydroxyl and a proton. The observed protrusions are definitely not charged, as no long range electrostatic interaction of the adsorbate with the tip is found. Therefore, water is either adsorbed as a molecule or subject to dissociation with the proton resting in the immediate vicinity of the remaining hydroxyl to preserve local charge neutrality. To identify the contrast of water related protrusions with either water molecules or a complex of a hydroxyl and an adjacent proton would require more sophisticated experiments in conjunction with extensive theoretical modelling of contrast formation. Both possible water related adsorbates can, however, be expected to be rather soft and flexible molecular configurations that can undergo severe deformation and relaxation during the strong interaction with the scanning tip. This explains the SFM contrast with adsorbates appearing as structureless protrusions extending over more than one lattice site.

In summary, we demonstrate that water even at room temperature and at very low exposures readily adsorbs on stoichiometric CeO₂(111). Molecules localize exclusively at cerium lattice sites and thus clearly identify this sub-lattice. Adsorption is dominated by molecule–surface interaction as neither clustering nor repulsion between adsorbates is observed. Water molecules are immobilised by an unexpectedly high diffusion barrier. The scanning tip is found to promote water adsorption, while adsorbed molecules suffer under severe deformation in the presence of the tip, which may eventually lead to induced diffusion.

Acknowledgments

We are grateful to F Esch, A Foster, A L Shluger, M Watkins and S Torbrügge for most stimulating discussions. Financial support by the Deutsche Forschungsgemeinschaft and the Stiftung Volkswagenwerk is gratefully acknowledged.

References

- [1] Thiel P A and Madey T E 1987 *Surf. Sci. Rep.* **7** 211
- [2] Henderson M A 2002 *Surf. Sci. Rep.* **46** 1
- [3] Meng S, Wang E G and Gao S W 2004 *Phys. Rev. B* **69** 195404
Nutt D R and Stone A J 2002 *J. Chem. Phys.* **117** 800
Meyer H, Entel P and Hafner J 2001 *Surf. Sci.* **488** 177
Morgenstern K and Rieder K-H 2002 *Chem. Phys. Lett.* **358** 250
Meyer B, Marx D, Dulub O, Diebold U, Kunat M, Langenberg D and Woell C 2004 *Angew. Chem. Int. Edn* **43** 6641
- [4] Henderson M A, Perkins C L, Engelhard M H, Thevuthasan S and Peden C H F 2003 *Surf. Sci.* **526** 1
- [5] Finocchi F and Goniakowski J 2001 *Phys. Rev. B* **64** 125426
Harris L A and Quong A A 2004 *Phys. Rev. Lett.* **93** 086105
- [6] Barth C and Reichling M 2001 *Nature* **414** 54
- [7] Trovarelli A 1996 *Catal. Rev. Sci. Eng.* **38** 439
- [8] Gritschneider S, Namai Y, Iwasawa Y and Reichling M 2005 *Nanotechnology* **16** S41
- [9] Gritschneider S and Reichling M 2007 in preparation
- [10] Zhuravlev L T 2000 *Colloids Surf. A* **173** 1
- [11] Gritschneider and Reichling M 2007 *Nanotechnology* **18** 044024
- [12] Redhead P A 1962 *Vacuum* **12** 203